

Coherent backscattering of neutrons

Jun-ichi Igarashi*

Department of Physics, University of California, Los Angeles, California 90024

(Received 30 December 1986)

We study the effects of multiple scattering on the elastic incoherent cross section of neutron backscattering. The cross section is found to be enhanced within a narrow cone centered around the backscattering direction. An antienhancement of intensities is predicted, provided that spin-flip scattering is dominant.

Recently, coherent backscattering of waves by random media has attracted much attention, after recent experiments¹⁻³ of light scattering showed that the scattered intensity is enhanced within a narrow cone centered around the backscattering direction. This enhancement is known to originate from the constructive interference between the time-reversed path and the original path for a backscattering geometry. It is closely related to Anderson localization, because the enhancement of backscattering intensity gives rise to a reduction of the diffusion constant. This comparison with Anderson localization was given by Khmelnitskii⁴ and Bergmann.⁵ Much theoretical work has already been done on the backscattering of light.⁶⁻¹⁰ In comparison with photons, coherent backscattering of neutrons has not yet been studied either experimentally or theoretically.

The first point that makes neutrons different from photons is that neutrons have a long mean-free path in ordinary materials. The mean free path can be estimated by $l \sim (1/4\pi |b|^2) V/N$, where b is the scattering length of the nuclei, V is the volume of the sample, and N is the number of nuclei that scatter neutrons. Using typical values, $V/N \sim (2 \text{ \AA})^3$ and $b \sim 10^{-4} \text{ \AA}$, l is of order 0.7 cm. Assuming that sample sizes are at most of order l , we expect that multiple-scattering effects come mainly from double scattering and the effect of localization is small. This does not mean of course that there is no coherent enhancement of the backscattering intensity. We will use the second-order Born approximation to calculate the backscattering intensities of neutrons which should be sufficient for lowest-order multiple scattering.

The second point that makes neutrons different from photons is that a neutron is a spin- $\frac{1}{2}$ particle and interacts with the nuclear spin. A spin-flip event, the flipping of a nuclear spin by a neutron, is equivalent to a measurement of position and can be expected to destroy coherence. The interaction between neutron and matter may be written as

$$U(\mathbf{r}) = \frac{2\pi\hbar^2}{m} \sum_i b_i \delta(\mathbf{r} - \mathbf{r}_i), \quad (1)$$

where m and \mathbf{r} are the mass and the position vector of the neutron, \mathbf{r}_i is the position vector of the i th nucleus, and b_i is a scattering amplitude operator defined by

$$b_i = A_i + \frac{1}{2} B_i \boldsymbol{\sigma} \cdot \mathbf{I}_i. \quad (2)$$

Here $\frac{1}{2} \boldsymbol{\sigma}$ is the spin operator of the neutron, and \mathbf{I}_i is the

nuclear spin operator of the i th nucleus. As will be shown later, if the spin-dependent part of the interaction is dominant, the backscattering intensity is suppressed by *destructive* interference, while only constructive interference is observed in light-scattering experiments.¹⁻³

We are interested in elastic incoherent scattering of neutrons with very long wavelength ($\lambda > 10 \text{ \AA}$). Bragg scattering does not occur in the backscattering direction for long wavelengths. We assume that the nuclear spins are pointing in random directions and that the nuclei are fixed at lattice points. Lattice vibrations may give rise to a reduction of intensities by the well-known Debye-Waller factor. This effect is expected, however, to be small at low temperatures for neutrons with long wavelength.

We first summarize the usual results of the first-order Born approximation. The cross section of elastic incoherent scattering is given by

$$\begin{aligned} \frac{d}{d\Omega} \sigma_i^{\text{tot}} &= \frac{d}{d\Omega} [\sigma_1(\uparrow \rightarrow \uparrow) + \sigma_1(\uparrow \rightarrow \downarrow)] \\ &= N[(\Delta A)^2 + \frac{1}{4} B^2 I(I+1)], \end{aligned} \quad (3)$$

with

$$A_i = A_0 + \delta A_i, \quad (\Delta A)^2 = \langle (\delta A_i)^2 \rangle_{\text{im}}, \quad (4)$$

$$B^2 I(I+1) = \langle B_i^2 I_i(I_i+1) \rangle_{\text{im}}, \quad (5)$$

where $\langle \dots \rangle_{\text{im}}$ denotes a configuration average, and $\sigma_1(\uparrow \rightarrow \uparrow)$ and $\sigma_1(\uparrow \rightarrow \downarrow)$ denote the non-spin-flip cross section and the spin-flip cross section, respectively. The polarization P' of the scattered neutrons is proportional to the incident polarization P , where $P = (I_1 - I_2)/(I_1 + I_2)$ with I_1, I_2 being the numbers of neutrons in \uparrow - and \downarrow -spin states, and the ratio is given by

$$\begin{aligned} P'/P &= \frac{d/d\Omega [\sigma(\uparrow \rightarrow \uparrow) - \sigma(\uparrow \rightarrow \downarrow)]}{d/d\Omega [\sigma(\uparrow \rightarrow \uparrow) + \sigma(\uparrow \rightarrow \downarrow)]} \\ &= \frac{(\Delta A)^2 - \frac{1}{12} B^2 I(I+1)}{(\Delta A)^2 + \frac{1}{4} B^2 I(I+1)}. \end{aligned} \quad (6)$$

We now discuss coherent backscattering due to double scattering using the second-order Born approximation. Figures 1 and 2 illustrate the processes of non-spin-flip transitions and spin-flip transitions, respectively. Process a in Fig. 1, for example, shows an incident neutron with spin \uparrow and momentum \mathbf{k}_i , which is scattered by nucleus j , changes its spin from \uparrow to \downarrow , propagates from the site j to l , is scattered by nucleus l , changes its spin from \downarrow to \uparrow ,

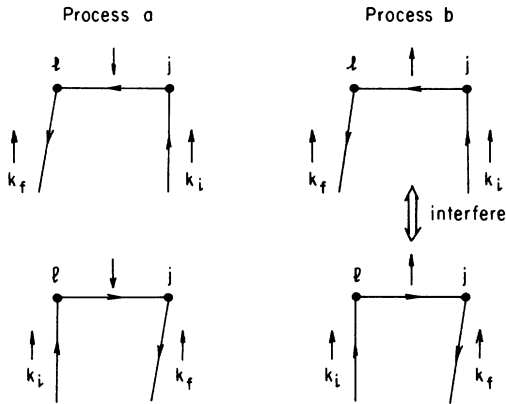


FIG. 1. Diagrams for non-spin-flip transitions. Solid lines indicate propagation of the neutron, where k_i and k_f are the incident and outgoing momentum, respectively. The arrows denote the spin states of the neutron. j and l denote nuclear positions where the neutron is scattered. Diagrams connected by double arrows interfere with each other near the backscattering situation.

and comes out with momentum k_f . The corresponding amplitude is given by

$$\psi_a^{jl} = \frac{1}{2} B_j \sqrt{(I_j + m_j + 1)(I_j - m_j)} \times \frac{1}{2} B_l \sqrt{(I_l + m_l)(I_l - m_l + 1)} \phi^{jl}, \quad (7)$$

with

$$\phi^{jl} = \exp(i\mathbf{k}_i \cdot \mathbf{r}_j) \frac{\exp(ik|\mathbf{r}_j - \mathbf{r}_l|)}{|\mathbf{r}_j - \mathbf{r}_l|} \exp(-i\mathbf{k}_f \cdot \mathbf{r}_l), \quad (8)$$

where $k = |\mathbf{k}_i| = |\mathbf{k}_f|$. The factor in front of ϕ^{jl} in Eq. (7) describes the transition matrix elements of the j th nuclear spin state from m_j to $m_j + 1$ and of the l th nuclear spin state from m_l to $m_l - 1$. Averaging over m_j and m_l , we find the contribution of this process to the cross section

$$\begin{aligned} \frac{d}{d\Omega} \sigma_2^a(\uparrow \rightarrow \uparrow) &= \sum_{\substack{j,l \\ (j < l)}} |\psi_b^{jl} + \psi_b^{lj}|^2 = [(\Delta A)^2 + \frac{1}{12} B^2 I(I+1)]^2 \sum_{j,l} \frac{1 + \cos(K|\mathbf{r}_j - \mathbf{r}_l|)}{|\mathbf{r}_j - \mathbf{r}_l|^2} \\ &= [(\Delta A)^2 + \frac{1}{12} B^2 I(I+1)]^2 N \left[\frac{N}{V} \right] (3\pi R) [1 + g_1(KR)], \end{aligned} \quad (11)$$

with

$$g_1(KR) = \frac{4}{3} \frac{\text{Si}(2KR)}{KR} - \frac{1 - (2/3)\cos(2KR)}{(KR)^2} + \frac{1}{3} \frac{\sin(2KR)}{(KR)^3} - \frac{1}{6} \frac{1 - \cos(2KR)}{(KR)^4}, \quad (12)$$

where $K = |\mathbf{k}_f + \mathbf{k}_i| = k\theta$ with θ the angle between \mathbf{k}_i and $-\mathbf{k}_f$, and $\text{Si}(x) = \int_0^x (\sin y/y) dy$. The asymptotic form of $g_1(KR)$ is given by

$$\begin{aligned} g_1(KR) &\sim \frac{2\pi}{3} \frac{1}{KR} + \dots \text{ for } KR \rightarrow \infty, \\ &\sim 1 - \frac{2}{27} (KR)^2 + \dots \text{ for } KR \rightarrow 0. \end{aligned} \quad (13)$$

The crossover between these forms occurs at $KR \sim 2\pi$. So the angular width of the enhancement is given by $\delta\theta \lesssim \lambda/R$, which is similar to the expression for photons where the mean free path ℓ of photons appears in place of R .^{9,10}

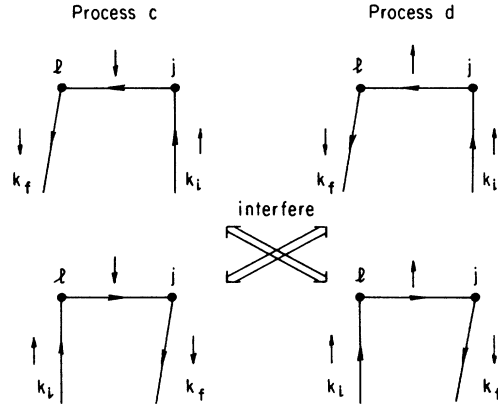


FIG. 2. Diagrams for spin-flip transitions.

as

$$\begin{aligned} \frac{d}{d\Omega} \sigma_2^a(\uparrow \rightarrow \uparrow) &= \sum_{j,l} |\psi_a^{jl}|^2 \\ &= \left[\frac{1}{6} B^2 I(I+1) \right]^2 \sum_{j,l} \frac{1}{|\mathbf{r}_j - \mathbf{r}_l|^2}. \end{aligned} \quad (9)$$

In this Rapid Communication, we assume that the sample has a spherical shape and we evaluate the lattice sum by using the continuum approximation. The result is

$$\sum_{j,l} \frac{1}{|\mathbf{r}_j - \mathbf{r}_l|^2} = N \left[\frac{N}{V} \right] (3\pi R),$$

where R is a radius of the sample.

The amplitude of process b (Fig. 1) is similarly given by

$$\psi_b^{jl} = (A_0 + \delta A_j + \frac{1}{2} B_j m_j)(A_0 + \delta A_l + \frac{1}{2} B_l m_l) \phi^{jl}. \quad (10)$$

Since process b does not give rise to any change of nuclear spin states, transition amplitudes ψ_b^{jl} and ψ_b^{lj} interfere with each other.¹¹ Among them, ψ_b^{jl} and ψ_b^{lj} have the same phase in the case of backscattering so they interfere constructively. Thus after a configurational average,¹¹ we find for the cross section

As for spin-flip transitions, there are two processes c and d (Fig. 2), whose amplitudes are given by

$$\psi_c^{jl} = \frac{1}{2} B_j \sqrt{(I_j + m_j + 1)(I_j - m_j)} (A_0 + \delta A_l - \frac{1}{2} B_l m_l) \phi^{jl}, \quad (14a)$$

$$\psi_d^{jl} = (A_0 + \delta A_j + \frac{1}{2} B_j m_j) \frac{1}{2} B_l \sqrt{(I_l + m_l + 1)(I_l - m_l)} \phi^{jl}. \quad (14b)$$

At first glance, one may think that there are no interference effects, because spin-flip transitions give rise to a change of nuclear spin states and thus contribute to incoherent scattering. However, interference effects *can* occur between ψ_c^{jl} and ψ_d^{jl} , because the same final state is realized after the scattering event. Note that for large B_l they have opposite phase so they interfere destructively. Averaging over m_j and m_l , we find for the cross section

$$\begin{aligned} \frac{d}{d\Omega} \sigma_2^{c+d}(\uparrow \rightarrow \downarrow) &= \sum_{j,l} |\psi_c^{jl} + \psi_d^{jl}|^2 \\ &= N \frac{N}{V} (3\pi R) \frac{1}{3} B^2 I(I+1) \{ (\Delta A)^2 + \frac{1}{12} B^2 I(I+1) + [(\Delta A)^2 - \frac{1}{12} B^2 I(I+1)] g_1(KR) \}. \end{aligned} \quad (15)$$

Note that when $(\Delta A)^2$ is smaller than $\frac{1}{12} B^2 I(I+1)$, the factor in front of $g_1(KR)$ is negative. It is this term that gives rise to antienhancement of the backscattering intensity due to interference between the scattering processes of Fig. 2.

Using Eqs. (9), (11), and (15), we find the multiple-scattering correction to the total cross section to be

$$\begin{aligned} \frac{d}{d\Omega} \sigma_2^{\text{tot}} &= \frac{d}{d\Omega} [\sigma_2^a(\uparrow \rightarrow \uparrow) + \sigma_2^b(\uparrow \rightarrow \uparrow) + \sigma_2^{c+d}(\uparrow \rightarrow \downarrow)] \\ &= N \frac{N}{V} (3\pi R) \{ [(\Delta A)^2 + \frac{1}{4} B^2 I(I+1)]^2 \\ &\quad + \{ [(\Delta A)^2 + \frac{1}{12} B^2 I(I+1)]^2 + \frac{1}{3} B^2 I(I+1) [(\Delta A)^2 - \frac{1}{12} B^2 I(I+1)] \} g_1(KR) \}. \end{aligned} \quad (16)$$

In Fig. 3, $(d/d\Omega) \sigma_2^{\text{tot}}$ is plotted as a function of KR , where the first term of Eq. (16) is normalized unity. When the nucleus has no spin [$B^2 I(I+1) = 0$], the enhancement of the cross section is maximal, since the destructive interference term is zero [the last term of Eq. (16)]. This situation is similar to light scattering experiments.¹⁻³ As the interaction between the neutron spin and nuclear spins becomes large, the destructive interference term grows larger and eventually overwhelms the constructive interference term and a dip appears. This reminds one of the effect of spin-orbit coupling in the weak localization of the electron which is also caused by destructive interference.⁵

The polarization of the scattered neutron is given by

$$\begin{aligned} \frac{P'}{P} &= \left(\frac{P'}{P} \right)_0 - \frac{N}{V} (3\pi R) \frac{\frac{1}{3} B^2 I(I+1)}{(\Delta A)^2 + \frac{1}{4} B^2 I(I+1)} \left\{ (\Delta A)^2 - \frac{1}{12} B^2 I(I+1) \right. \\ &\quad \left. + \frac{(\Delta A)^2 - \frac{1}{4} B^2 I(I+1)}{(\Delta A)^2 + \frac{1}{4} B^2 I(I+1)} [(\Delta A)^2 + \frac{1}{12} B^2 I(I+1)] g_1(KR) \right\}, \end{aligned} \quad (17)$$

where $(P'/P)_0$ represents the result of the first-order Born approximation. In Fig. 4, we show the calculated results of P'/P as a function of KR , using the typical values, $(\Delta A)^2 + \frac{1}{4} B^2 I(I+1) = (10^{-4} \text{ \AA})^2$, $R = 4 \times 10^6 \text{ \AA}$, $V/N = (2 \text{ \AA})^3$. If we have no nuclear spin, then the polarization of the scattered neutron should be the same as the incident polarization ($P'/P = 1$). When the interaction between the neutron spin and nuclear spins grows large, P'/P deviates from the results of the first-order Born approximation and is enhanced in the backscattering direction.

We now comment on the possibility of experimental realizations. To observe the effect of double scattering, a large sample is favorable, because the ratio of the total cross section due to double scattering to that due to single scattering is proportional to a sample size; the ratio is

$$\sigma_2^{\text{tot}} / \sigma_1^{\text{tot}} = \frac{N}{V} (3\pi R) [(\Delta A)^2 + \frac{1}{4} B^2 I(I+1)].$$

On the other hand, to observe coherent enhancement of backscattering intensities over appreciable angles near the

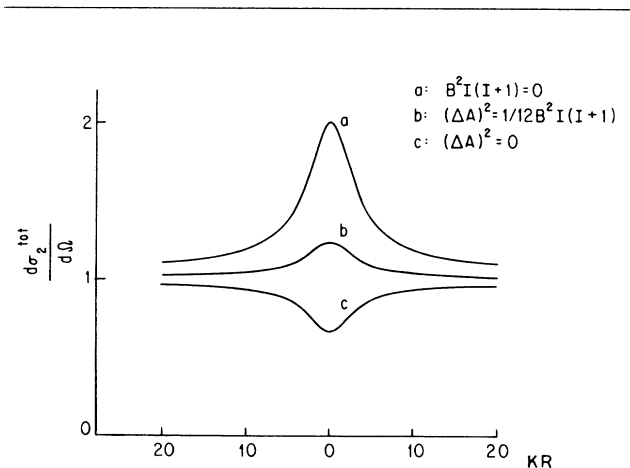


FIG. 3. The multiple-scattering correction $(d/d\Omega) \sigma_2^{\text{tot}}$ to the total cross section as a function of KR . The first term of Eq. (16) is normalized to unity. Curve a : $B^2 I(I+1) = 0$, b : $(\Delta A)^2 = \frac{1}{12} B^2 I(I+1)$, c : $(\Delta A)^2 = 0$.

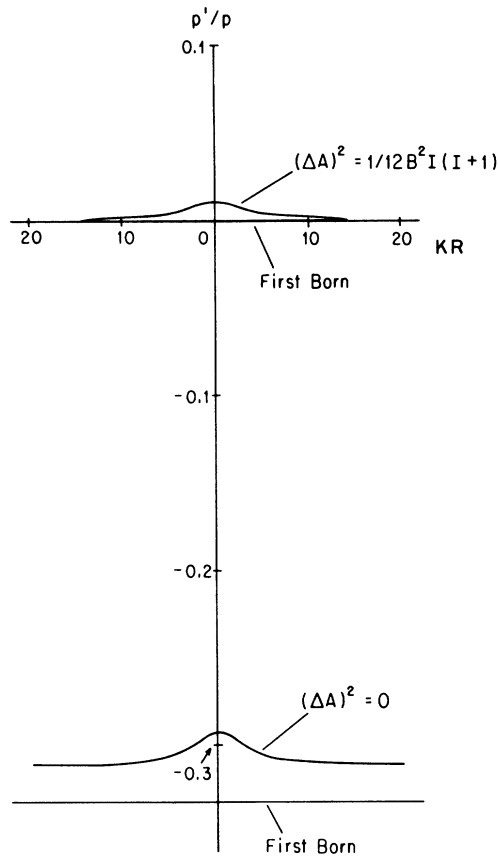


FIG. 4. The ratio of the polarization of the scattered neutron to that of the incident neutron as a function of KR , by using the typical values, $(\Delta A)^2 + \frac{1}{4} B^2 I(I+1) = (10^{-4} \text{ \AA})^2$, $R = 4 \times 10^6$ \AA , and $V/N = (2 \text{ \AA})^3$. The straight lines with "First Born" represent the results of the first-order Born approximation.

backscattering situation, a small sample and a large wavelength of neutrons are favorable, because the angular width can be estimated as $\delta\theta \lesssim \lambda/R$. Neutron optics has developed so rapidly over recent years¹² that it would be possible to use ultra-cold-neutrons with a wavelength $\lambda \sim 400 \text{ \AA}$. In this case, if $R \sim 4 \times 10^6 \text{ \AA}$, then $\delta\theta \sim 10^{-4}$ rad and $\sigma_2^{\text{tot}}/\sigma_1^{\text{tot}} \sim 4.7 \times 10^{-2}$ for $V/N = (2 \text{ \AA})^3$ and $(\Delta A)^2 + \frac{1}{4} B^2 I(I+1) = (10^{-4} \text{ \AA})^2$. If the sample is smaller than this, $\delta\theta$ increases, while $\sigma_2^{\text{tot}}/\sigma_1^{\text{tot}}$ decreases. What substances are suitable to experiment? Magnetic atoms must be excluded, because our theory has neglected the effects of magnetic scattering due to the interaction between the magnetic moment of neutrons and that of atoms, which is large for magnetic atoms. Compounds of hydrogen may be better, because the nucleus has a large incoherent (spin-flip) cross section.

In summary, we have found that the elastic incoherent cross section is enhanced near the backscattering direction due to interference effects. If we compare neutron backscattering enhancement with photon backscattering enhancement, then a difference arises because neutrons have a long mean free path so only double scattering is relevant, and because antienhancement occurs if the interaction between neutron spin and nuclear spins is dominant. The spin effects would be complicated when multiple scattering higher than double scattering is effective in large samples. For light, the polarization effects may play a role similar to the spin effects of neutrons in anisotropic media which, for example, contain optically active substances. The analysis of these cases is left for the future.

The author wishes to thank Professor R. Bruinsma for many stimulating discussions and for a critical reading of the manuscript. The author is grateful to the University of California at Los Angeles and IBM for financial support.

*Permanent address: Department of Physics, Osaka University, Toyonaka, Osaka 560, Japan.

¹Y. Kuga and A. Ishimaru, *J. Opt. Soc. Am. Ser. A* **8**, 831 (1984).

²M. P. van Albada and A. Lagendijk, *Phys. Rev. Lett.* **55**, 2692 (1985).

³P. E. Wolf and G. Maret, *Phys. Rev. Lett.* **55**, 2696 (1985).

⁴D. E. Khmel'nitski, *Physica B&C* **126**, 235 (1984).

⁵G. Bergmann, *Phys. Rev. B* **28**, 2914 (1983).

⁶K. M. Watson, *J. Math. Phys.* **10**, 688 (1969).

⁷A. A. Golubentsev, *Zh. Eksp. Teor. Fiz.* **86**, 47 (1984) [*Sov. Phys. JETP* **59**, 26 (1984)].

⁸L. Tsang and A. Ishimaru, *J. Opt. Soc. Am. Ser. A* **8**, 836 (1984); *ibid.* **8**, 1331 (1985).

⁹E. Akkermans, P. E. Wolf, and R. Maynard, *Phys. Rev. Lett.*

56, 1471 (1986).

¹⁰M. J. Stephen, *Phys. Rev. Lett.* **56**, 1809 (1986).

¹¹In crystals, for $k_f - k_i = G$ (a reciprocal vector) and $r_j - r_l = r_{j'} - r_{l'}$, the terms with the factor A_δ^2 in $\psi_\delta^{j'}$ and $\psi_\delta^{l'}$ have the same phase and interfere constructively with each other and give rise to a correction to the coherent cross section. The terms containing the factors δA_j , δA_l , $\delta A_{j'}$, and $\delta A_{l'}$ give rise to intensity fluctuations, because the configurational average is not justified. In order to suppress such fluctuations, it is better to use liquid samples or to rotate samples in experiments. For intensity fluctuations in light, see M. Kaveh, M. Rosenbluh, I. Edrei, and I. Freund, *Phys. Rev. Lett.* **57**, 2049 (1986).

¹²For a review, see A. G. Klein and S. A. Werner, *Rep. Prog. Phys.* **46**, 259 (1983).